Contrasting Chlorine Chemistry on Volcanic and Wildfire Aerosols 1 in the Southern Mid-Latitude Lower Stratosphere 2 Peidong Wang¹ and Susan Solomon¹ 3 ¹Department of Earth, Atmospheric, and Planetary Sciences, Massachusetts Institute of 4 Technology, Cambridge, MA, USA 5 Corresponding author: Peidong Wang (pdwang@mit.edu) 6 **Key Points:** 7 8 The tracer-tracer correlation method reveals chemical perturbations associated with 9 volcanic aerosols or smoke 10 The 1991 Pinatubo eruption and the 2020 Australian wildfire markedly perturbed HCl in 11 the southern mid-latitude lower stratosphere 12

13

14

similar decreases in HCl

The Pinatubo eruption had 10 times more aerosol loading than the Australian wildfire, but

Abstract

- Volcanic eruptions and wildfires can impact stratospheric chemistry. We apply tracer-tracer
- 17 correlations to satellite data from ACE (Atmospheric Chemistry Experiment Fourier Transform
- Spectrometer) and HALOE (The HALOgen occultation Experiment) at 68 hPa to consistently
- compare the chemical impact on HCl after multiple wildfires and volcanic eruptions of different
- 20 magnitudes. The 2020 Australian New Year (ANY) fire displayed an order of magnitude less
- stratospheric aerosol extinction than the 1991 Pinatubo eruption, but showed similar large
- changes in mid-latitude lower stratosphere HCl. While the mid-latitude aerosol loadings from the
- 23 2015 Calbuco and 2022 Hunga volcanic eruptions were similar to the ANY fire, little impact on
- 24 HCl occurred. The 2009 Australian Black Saturday (ABS) fire and 2021 smoke remaining from
- 25 2020 yield small HCl changes, at the edge of the detection method. These observed contrasts
- 26 across events highlight greater reactivity for smoke versus volcanic aerosols at warm
- temperatures.

28 29

15

Plain Language Summary

- An unprecedented change in HCl was observed in the lower stratosphere after the 2020
- Australian New Year (ANY) wildfire using satellite records since 2004. In this study, we
- conduct a consistent analysis of HCl impacts using an additional satellite product with
- measurements since 1991 to examine effects of the catastrophic 1991 Pinatubo volcanic eruption
- and smaller eruptions, and compare them to the 2020 ANY fire (and remaining smoke in 2021),
- as well as the much smaller 2009 Australian Black Saturday (ABS) bushfire. This allows
- analysis of different types of particles (smoke versus volcanic) and the extremes of each
- observed to date. While the Pinatubo eruption displayed 10 times greater aerosol loading in the
- stratosphere than the ANY fire, these two events led to similar net chemical changes in HCl. In
- 39 contrast, no significant changes in HCl were observed in the lower stratosphere following the
- 40 Hunga and Calbuco volcanic eruptions, which displayed similar levels of extinction to ANY.
- Small effects were observed from ABS fire and in 2021, allowing identification of the lower
- limit of the amount of smoke affecting HCl. These contrasts between events indicate that the
- wildfire smoke aerosols must be more reactive insofar as chlorine chemistry is concerned.

1 Introduction

The southern hemisphere stratosphere has been perturbed by major aerosol injection events frequently in the past several years, associated with stratospheric ozone depletion. The April 2015 Calbuco volcanic eruption injected about 0.3 Tg of SO₂ into the stratosphere (Pardini et al., 2018), contributing to a record-large ozone hole in October of that year (Solomon et al., 2016). The 2019-2020 Australian New Year wildfire (ANY) injected about 1 Tg of smoke particles into the stratosphere (Peterson et al., 2021), and was followed by significant perturbations in mid-latitude chemistry (Bernath et al., 2022; Santee et al., 2022; Solomon et al., 2023), and an extended Antarctic ozone hole season (Ansmann et al., 2022; Ohneiser et al., 2022; Chipperfield and Bekki, 2024). The January 2022 Hunga Tonga-Hunga Ha'apai (Hunga) underwater volcanic eruption injected around 0.4 Tg of SO₂ (Carn et al., 2022) along with ~150 Tg of H₂O (Millán et al., 2022) into the stratosphere, and led to record low mid-latitude O₃ at some altitudes as well as significant polar O₃ depletion (Santee et al., 2023; Wang, X. et al., 2023; Wilmouth et al., 2023; Wohltmann et al., 2024; Zhang et al., 2024).

Volcanic eruptions can deplete stratospheric O₃ via various heterogeneous reactions. In the polar region where the temperature can be low, SO₂ from volcanic eruptions increases sulfate aerosols and subsequently can provide more surface area for chlorine to activate from reservoir species (mainly HCl and ClONO₂, or Cly) and deplete O₃, particularly in cold air at the edge of the polar vortex (Solomon et al., 2016). In the mid-latitude region, temperatures are generally too warm for sulfate to take up HCl efficiently (Hanson and Ravishankara, 1993; Shi et al., 2001). Instead, mid-latitude O₃ depletion after volcanic eruptions is mainly due to N₂O₅ hydrolysis that reduces NOx, modulates ClO/ClONO₂ partitioning, and indirectly depletes O₃ (Solomon et al., 1996). Heterogeneous mid-latitude chemistry also depends on water vapor partial pressure (Solomon, 1999). With a large amount of H₂O emitted from Hunga, several key heterogeneous reactions can also happen more efficiently at warmer temperatures; this effect contributed to the record low mid-latitude O₃ observed in 2022 (Zhang et al., 2024).

What makes wildfire different from volcanic eruptions is that organic aerosol makes up a large portion of the smoke composition (Murphy et al., 2021). The uptake of HCl on organic aerosols is orders of magnitude more efficient than on sulfate aerosols at temperatures warmer than \sim 200 K (Solomon et al., 2023). The high solubility of HCl on organics at warm temperatures means that chlorine activation is no longer limited to polar winter and spring. N₂O₅ hydrolysis also likely contributed to mid-latitude O₃ depletion after the 2020 ANY fire, but this mechanism alone cannot explain the unprecedented changes observed in Cly in 2020 (Solomon et al. 2022; 2023). More evidence, especially from laboratory studies, is needed to verify the hypothesized reaction rates on different types of aerosols (Chipperfield and Bekki, 2024).

In this paper, we focus on chlorine processing in the southern mid-latitudes during the fall to winter season (March to July). This period follows the Australian summer wildfire season, and displayed unprecedented changes in stratospheric Cly after the ANY fire from MLS (Microwave Limb Sounder, 2004-present) and ACE (Atmospheric Chemistry Experiment - Fourier Transform Spectrometer, 2004-present) satellite data (Bernath et al., 2022; Santee et al., 2022). In an earlier study by Wang, P. et al. (2023), we used a tracer-tracer method to derive the chemical impact on Cly from satellite data after the ANY fire. Here we use a similar method to look for stratospheric chemical impacts on HCl after the 2009 Australian Black Saturday (ABS) bushfire. While this was a much smaller wildfire compared to the 2020 ANY fire, several biomass indicators observed from satellite suggest that the wildfire plume indeed reached the

- lower stratosphere (Glatthor et al., 2013), and injected up to 0.1 Tg of aerosol into the
- stratosphere (Peterson et al., 2021). We also leverage satellite data from HALOE (The HALOgen
- occultation Experiment) onboard the UARS (Upper Atmosphere Research Satellite) to examine
- 92 the changes in HCl after the catastrophic 1991 Pinatubo eruption, which injected up to ~19 Tg of
- SO₂ (Guo et al., 2004). The long composite record from HALOE and ACE spanning more than
- 94 three decades allows consistent comparison of the chemical impacts of wildfire and volcanic
- aerosols, for these identified wildfire events that have reached the lower stratosphere, as well as
- multiple smaller volcanic eruptions (including Calbuco in 2015 and Hunga in 2022), and the
- 97 1991 Pinatubo eruption, the largest volcanic eruption in the satellite era.

2 Data and Methods

2.1 ACE and HALOE satellite data

ACE version 5.2 (Bernath, 2005) and HALOE version 19 (Russell et al., 1993) are used in this study. Both ACE and HALOE are infrared solar occultation instruments, providing vertical profiles at sunset and sunrise. HALOE data are available from 1991 to 2005, and ACE data are available from 2004 to present. In the lower stratosphere, HALOE and ACE agree reasonably well for temperature and multiple trace gases, except for NO₂ (McHugh et al., 2005). Here we present results in mid-latitude, defined as 30-45S. We picked this latitude range because both HALOE and ACE provide similar sampling distributions there, and this region is less affected by the air coming from the polar region than higher latitudes would be. Figure 1A-C shows mid-latitude monthly averaged temperature, CH₄, HCl, and aerosol extinction, linearly interpolated in log pressure to 68 hPa. In 2004-2005 when measurements are available from both instruments, HALOE and ACE show broadly consistent results.

Aerosol extinction from HALOE is available at four different channels (2.45, 3.4, 3.46, and 5.26 μ m). Data at 2.45 and 5.26 μ m are strongly biased after Pinatubo and are not recommended for scientific use, and 3.4 μ m is also affected slightly by failure to remove NO₂ absorption (Thomason, 2012). ACE aerosol extinction is available at two channels (525 and 1020 nm). To facilitate direct comparisons between ACE and HALOE, we converted HALOE aerosol extinction from 3.46 μ m to 1020 nm. Following Thomason (2012), we applied two sets of scaling factors to HALOE aerosol extinction (0.2 \pm 0.05 before 1997 and 0.375 \pm 0.125 after 1997) derived from the HALOE and SAGE II (Stratospheric Aerosol and Gas Experiment II) 3.46 μ m to 1020 nm ratios (the spreads in the scaling factors are represented as gray shadings in Figure 1D). This method appears to work well and does not require prior assumptions on the particle size distribution. The 1020 nm aerosol extinction derived from HALOE in this way and the direct retrieval from ACE show consistent results in the overlap period during 2004-2005 and are consistent with the zonal mean 1020 nm aerosol extinction product from the GloSSAC (Global Space-based Stratospheric Aerosol Climatology version 2.21; NASA/LARC/SD/ASDC, 2023) averaged for a similar latitude range at 18.5 km (dashed black line in Figure 1D).

2.2 Tracer-tracer correlation method

Both ACE (using high resolution infrared absorption in solar occultation) and HALOE (using a lower-resolution infrared emission band) measure HCl, aerosol extinction, and several other trace gases simultaneously, allowing a quantitative estimate of the change in HCl

associated with aerosol abundances at individual satellite overpasses. However, the observed 130 mixing ratio of HCl reflects both dynamic and chemical influences. Here we use CH₄ as a 131 dynamical tracer observed by both instruments and exploit the HCl-CH₄ correlation in the mid-132 latitude during fall/early winter season (March-July) to search for chemical impacts. Individual 133 points in Figure 2 represent co-located CH₄ and HCl satellite measurements that are linearly 134 detrended (discussed later). Following Wang, P. et al. (2023), we first construct a "no-chemistry" 135 baseline based on the March CH₄-HCl relationship composite for all the background years 136 without major wildfires or volcanic eruptions. For HALOE data, this baseline covers 1997-2005 137 and for ACE data, it spans 2004-2019 (excluding 2009 and 2015-2016), shown as thick blue and 138 orange lines in Figure 2, respectively. The shaded areas in Figure 2 represent the full range of the 139 140 CH₄-HCl relationship derived from individual background years, capturing interannual variability, which is a key source of baseline uncertainty (Wang, P. et al., 2023). Overall, the 141 CH₄-HCl relationships from both satellites are consistent with each other. We define Δ HCl as the 142 departure of HCl in individual data points from the "no-chemistry" baseline, which largely 143 describes the net chemical change in HCl. In the absence of chemical changes, a plot of HCl 144 versus CH₄ should follow a straight line, with dynamical changes moving along but not 145 departing from the line (this is more clearly shown in the ACE data due to its high precision). 146

The inactive tracer used in this study to derive ΔHCl is CH₄. Both HCl and CH₄ from HALOE use gas filter radiometry, so the retrievals are generally insensitive to high aerosol loading after the Pinatubo eruption (Hervig et al., 1995). HALOE HCl and CH₄ have previously been used in tracer-tracer analysis after Pinatubo given that the relative error between these tracers is less than 5%, although the first half of 1992 could still be affected by the extreme aerosol loading (Dessler et al., 1997). For consistency, we also use CH₄ as the inactive tracer in HALOE ACE data in this study. CH₄ and HCl come from different emission sources, and different trends may bias ΔHCl calculation, especially in such a three-decade-long satellite record. We therefore linearly detrended CH₄ and HCl fitted from 1997-2005 in HALOE and 2004-2018 in ACE. We considered the use of HF as an inactive tracer in this analysis, although the high aerosol loads of Pinatubo may influence the HALOE retrieval (Thomason, 2012). Figure S1 compares ΔHCl in the ACE record calculated from CH₄ and from HF, which is much more inert than CH₄ in the lower stratosphere. For the background years, most of the data are clustered around 0, and for years after major volcanic eruptions and wildfires, the two inactive tracers resulted in similar Δ HCl. Overall, CH₄-derived Δ HCl has a low bias by 0.01 ppb compared to HF-derived ΔHCl.

3 Results

147

148

149150

151

152

153

154

155

156

157

158

159

160

161

162

163

164165

166

167

168

169

170

171172

173

Figure 3 shows satellite-derived mid-latitude ΔHCl at 68 hPa as a function of the 1020 nm aerosol extinction in the years after the Pinatubo, Calbuco, Hunga volcanic eruptions, and the ABS and the ANY fires (labeled by different colors and markers shown in the figure legend). The gray dots are for example background years in 2000 (from HALOE) and the black dots are for the background year 2012 (from ACE), as these two years do not have known major volcanic eruptions or large wildfires. The larger background ΔHCl spread in 2000 compared to 2012 can be partially due to lower precision in HALOE compared to ACE. Since HCl becomes much more soluble on volcanic aerosols at temperatures colder than ~195 K (Hanson and Ravishankara, 1993; Shi et al., 2001; Solomon et al., 2023), to prevent misinterpreting the temperature for chlorine processing on different aerosol types after volcanic eruptions and wildfires, ΔHCl in

Figure 3 is separated into five temperature regimes (<=195 K, 195-200 K, 200-205 K, 205-210 174 K, and > 210 K) based on the air parcel's recent minimum temperature exposure (instead of 175 using the temperatures directly observed at the time of the satellite overpasses). Following 176 Wang, P. et al. (2023), at each satellite overpass, we run a 5-day back trajectory calculation using 177 Lagranto (Lagrangian Analysis Tool; Sprenger and Wernli, 2015) driven by the ERA5 (fifth 178 generation atmospheric reanalysis product from the European Centre for Medium-Range 179 Weather Forecasts; Herbach et al., 2020) meteorology. Figure S2 is comparable to Figure 3 but 180 instead uses the satellite-observed temperature directly. Generally, because the latitude range we 181 choose is far away from the polar region, most of the data points are not recently exposed to 182 substantially colder temperatures, and can well represent warm mid-latitude conditions. 183

184

185

186

187 188

189 190

191

192

193 194

195

196

197

198

199

200

201

202

203

204

205

206

207

208

209

210

211

212

213

214

215

216

217

218

The main focus here is on the strong negative values of Δ HCl, indicating efficient uptake of HCl on particles, especially at temperatures warmer than 200 K when PSCs are very unlikely to occur (McCormick et al., 1982). Using the ACE record from 2004-2023, aerosol extinction after the Calbuco and Hunga volcanic eruptions reached a similar (or even higher) value to that of the ANY fire, which is about an order of magnitude higher than background conditions. However, only the two consecutive years in this record after the ANY fire show a noticeable HCl decrease due to chemistry, where Δ HCl falls outside the uncertainty range (characterized by the full range of interannual variability in background years during ACE record, represented as the orange shading in Figure 3). This is consistent with Solomon et al. (2023), who suggested that the organic aerosols from wildfires are orders of magnitude more efficient in uptaking HCl compared to volcanic aerosols under warm mid-latitude temperatures. We can only find a similar degree of change in HCl after the 1991 Pinatubo eruption. However, the aerosol extinction in 1992 reached $\sim 10^{-2}$ km⁻¹, which is more than one order of magnitude higher than the ANY fire. Given significantly larger aerosol amounts, the decrease in HCl after the Pinatubo eruption is mainly due to enhanced N2O5 hydrolysis and therefore elevated HOx depleting HCl (Kinnison et al., 1994). The 2009 ABS fire led to a small enhancement in aerosol extinction that is close to 2021 conditions. There are a few data points in 2009 that displayed Δ HCl lower than the ACE uncertainty range (yellow triangles in Figure 3). Figure S3 shows the tracer-tracer scatter plot in ACE that highlights the ABS fire color-coded by CO, which is an indicator for biomass burning. The low ΔHCl points in 2009 are mainly in March, and are associated with high CO concentrations, suggestive of some role for wildfire chemistry. However, this chemical impact is small, barely outside the range of other years, and did not last long; the Δ HCl in 2009 falls within the uncertainty range quickly after March.

Hunga volcanic aerosols were accompanied by significant H₂O injection and have higher extinction than Calbuco and the ANY fire (Zhu et al., 2022). Interestingly, even though 2022-23 after the Hunga eruption and 1994 (3 years after the Pinatubo eruption) show comparable amounts of aerosol extinction at 68 hPa, less ΔHCl was found after the Hunga eruption. Although it is worth noting that the altitude associated with the largest change in aerosol extinction and HCl after the Hunga eruption is at a higher altitude (Wang, X. et al., 2023; Wilmouth et al., 2023). A caveat of considering aerosol extinction alone for indications of heterogeneous reaction is that particle size distribution is overlooked. Further, different types of aerosols may exhibit different optical properties, affecting extinction values (Ohneiser et al., 2022). Particle diameter after the Hunga eruption reached ~0.56 μm (Asher et al., 2023), just at the peak of scattering efficiency (Murphy et al., 2021; Li et al., 2024); this event therefore resulted in higher aerosol extinction given relatively lower mass of aerosols. On the contrary,

particles after the Pinatubo eruption reached a diameter larger than 0.7 µm (Wilson et al., 2008), 219 decreasing their scattering efficiency. Therefore, the mass of aerosols in 1994 may be much 220 higher than 2022-23, despite displaying a similar level of aerosol extinction. Likewise, the mean 221 diameter after the ANY fire was smaller compared to that of Hunga (Ansmann et al., 2021), 222 suggesting given similar aerosol extinctions that the mass of ANY aerosols is also larger than 223 Hunga. Particle sizes are also important in determining the decay time of these aerosols in the 224 stratosphere, contributing to how long these aerosols can affect stratospheric chemistry over time 225 (Ohneiser et al., 2022). 226

Figure 4 averages the net chemical impact on HCl in various aerosol extinction bins for the wildfire years (which contain more organic aerosols, with red lines showing the ANY fire, and yellow lines for the ABS fire) and all other years in 1992 to 2023 (including volcano and background years, which mainly contain inorganic sulfates). We composite all the satellite data in 30-45S (without filtering out data points with low temperatures) because the latitude range we choose here is equatorward enough to prevent significant PSC-induced Cl activation (there are only a few points that had 5-day minimum temperature below 195 K based on the back trajectory calculation in Figure 3).

After the catastrophic 1991 Pinatubo eruption, it took about 4 years for aerosol extinctions to decay to a level similar to the ANY fire. The magnitude of Δ HCl also shows a consistent decay associated with the decay in aerosol extinction after Pinatubo. The net chemical impact on HCl from the Pinatubo eruption vanishes in 1995 when the average aerosol extinction reaches ~5×10⁻⁴ km⁻¹. For the Calbuco eruption and background years, when the aerosol extinctions were smaller than 5×10^{-4} km⁻¹, insignificant changes in Δ HCl were observed. The Hunga eruption boosted the aerosol extinction to $\sim 10^{-3}$ km⁻¹, but has only a minor impact on Δ HCl, likely due to less surface area compared to Pinatubo aerosols; the Δ HCl curve is hence close to zero at $\sim 10^{-3}$ km⁻¹. Along the Δ HCl versus aerosol extinction curve, the net chemical change in HCl during wildfire year in 2020 is a clear outlier compared to the background and volcanic years. In 2021, wildfire aerosols are transported further poleward, and the chemical impact at 30-45S becomes smaller (although there is still significant Cl activation in 2021 at 40-55S and 65-90S shown in Wang, P. et al. 2023). This difference in HCl uptake is also broadly consistent with the difference in ozone loss after the ANY fire and the Calbuco and Pinatubo eruptions (Ansmann et al., 2022). The 2009 ABS fire, due to its small magnitude (only a-tenth of the stratospheric aerosol loading compared to the ANY fire), may have led to a small decrease in the mean Δ HCl but it is close to the uncertainty range. At the latitude range we chose, both 2009 and 2021 have similar aerosol extinction and display a similar impact on ΔHCl that is on the lower end of the background/volcano range. The two events suggest that significant mid-latitude wildfire impacts on HCl outside of the range of variability at these latitudes would require extinction levels of about ~a few × 10⁻⁴ km⁻¹ or larger.

4 Conclusions

227

228

229

230

231

232

233

234

235

236

237

238

239

240

241

242

243

244

245

246

247

248

249250

251252

253

254

255

256

257

258

259

260

261

The 2020 ANY fire, the largest wildfire since the satellite era, injected a large amount of aerosol into the lower stratosphere and resulted in an unprecedented change in HCl and ClONO₂ relative to MLS and ACE records from 2004 to 2023. In an earlier study from Wang, P. et al. (2023), we quantified the net chemical impact on HCl after the ANY fire from satellite data using the tracer-tracer method. Here, we use this method to consistently combine satellite

observations from ACE (2004-2023) and HALOE (1992-2005), and thereby examine the net chemical impacts in HCl after another smaller wildfire in 2009 (Black Saturday bushfire) as well as the ANY fire as compared to a series of volcanic eruptions of different sizes – from the recent 2015 Calbuco and 2022 Hunga eruption to the catastrophic 1991 Pinatubo eruption.

The approach we used allows consistent identification of volcanic impacts on midlatitude HCl in the lower stratosphere for several years after Pinatubo. Direct satellite evidence suggests a similar degree of net HCl decrease (after removing the dynamical impacts) after the ANY fire and the Pinatubo eruption at 68 hPa, despite Pinatubo having an order of magnitude higher aerosol extinction than the ANY fire. The decrease in mid-latitude HCl after the Pinatubo eruption is thought to be due to enhanced gas phase reaction with OH (given significant reductions in NOx through N₂O₅ hydrolysis and therefore HOx enhancement; Kinnison et al., 1994). However, wildfires containing a significant portion of organic aerosols (Murphy et al., 2021) can dissolve HCl more efficiently at warm temperatures (Solomon et al., 2023), facilitating the reaction between ClONO₂ and HCl while suppressing ClONO₂ hydrolysis. Therefore, only a relatively small amount of wildfire aerosols in the stratosphere might cause chemical changes in HCl. The unprecedented change in chlorine species after the 2020 ANY fire has increased attention on the impact of wildfires in the stratosphere. Earlier wildfires with smaller magnitudes could also affect stratospheric chlorine activation but may have been overlooked. Here we see some evidence suggesting that the much smaller 2009 ABS bushfire may have impacted the stratospheric chlorine chemistry in the southern hemisphere mid-latitude lower stratosphere, but only at the edge of variability. We used the 2009 wildfire event and the decay of the 2020 wildfire smoke to the year 2021 to suggest that significant mid-latitude wildfire impacts on HCl outside the range of variability at the latitudes explored here would require extinction levels higher than these events, or above about \sim a few \times 10⁻⁴ km⁻¹. Applying the method developed here to a wider range of altitudes, latitudes, and events in both hemispheres is a topic for future work.

Acknowledgments

262

263

264

265

266

267

268269

270

271

272

273

274

275

276

277

278

279

280

281 282

283

284

285

286

287

288

290

291

292

295

296

P.W. and S.S. gratefully acknowledge support by NSF-AGS [2316980 and 2128617].

Open Research

- HALOE and ACE-FTS data are freely available at https://haloe.gats-inc.com/home/index.php and
- 293 http://www.ace.uwaterloo.ca, respectively. Data and code used in this manuscript are available on Zenodo at
- 294 https://doi.org/10.5281/zenodo.13387165 (Wang, 2024).

References

297	Ansmann, A., Ohneiser, K., Chudnovsky, A., Knopf, D. A., Eloranta, E. W., Villanueva, D., et
298	al. (2022). Ozone depletion in the Arctic and Antarctic stratosphere induced by wildfire
299	smoke. Atmospheric Chemistry and Physics, 22(17), 11701–11726.
300	https://doi.org/10.5194/acp-22-11701-2022
301	Ansmann, A., Ohneiser, K., Mamouri, RE., Knopf, D. A., Veselovskii, I., Baars, H., et al.
302	(2021). Tropospheric and stratospheric wildfire smoke profiling with lidar: mass, surface
303	area, CCN, and INP retrieval. Atmospheric Chemistry and Physics, 21(12), 9779–9807.
304	https://doi.org/10.5194/acp-21-9779-2021
305	Asher, E., Todt, M., Rosenlof, K., Thornberry, T., Gao, RS., Taha, G., et al. (2023).
306	Unexpectedly rapid aerosol formation in the Hunga Tonga plume. Proceedings of the
307	National Academy of Sciences, 120(46), e2219547120.
308	https://doi.org/10.1073/pnas.2219547120
309	Bernath, P. F. (2005). Atmospheric Chemistry Experiment (ACE): Mission overview.
310	Geophysical Research Letters, 32(15), L15S01. https://doi.org/10.1029/2005GL022386
311	Bernath, P., Boone, C., & Crouse, J. (2022). Wildfire smoke destroys stratospheric ozone.
312	Science, 375(6586), 1292-1295. https://doi.org/10.1126/science.abm5611
313	Carn, S. A., Krotkov, N. A., Fisher, B. L., & Li, C. (2022). Out of the blue: Volcanic SO2
314	emissions during the 2021–2022 eruptions of Hunga Tonga—Hunga Ha'apai (Tonga).
315	Frontiers in Earth Science, 10, 976962. https://doi.org/10.3389/feart.2022.976962
316	Chipperfield, M. P., & Bekki, S. (2024). Opinion: Stratospheric ozone – depletion, recovery and
317	new challenges. Atmospheric Chemistry and Physics, 24(4), 2783–2802.
318	https://doi.org/10.5194/acp-24-2783-2024

Dessler, A. E., Considine, D. B., Rosenfield, J. E., Kawa, S. R., Douglass, A. R., & Russell, J. 319 M. (1997). Lower stratospheric chlorine partitioning during the decay of the Mt. Pinatubo 320 aerosol cloud. Geophysical Research Letters, 24(13), 1623–1626. 321 https://doi.org/10.1029/97GL01470 322 Glatthor, N., Höpfner, M., Semeniuk, K., Lupu, A., Palmer, P. I., McConnell, J. C., et al. (2013). 323 324 The Australian bushfires of February 2009: MIPAS observations and GEM-AQ model results. Atmospheric Chemistry and Physics, 13(3), 1637–1658. 325 https://doi.org/10.5194/acp-13-1637-2013 326 Guo, S., Bluth, G. J. S., Rose, W. I., Watson, I. M., & Prata, A. J. (2004). Re-evaluation of SO2 327 release of the 15 June 1991 Pinatubo eruption using ultraviolet and infrared satellite 328 sensors. Geochemistry, Geophysics, Geosystems, 5(4), 2003GC000654. 329 https://doi.org/10.1029/2003GC000654 330 Hanson, D. R., & Ravishankara, A. R. (1993). Uptake of hydrochloric acid and hypochlorous 331 acid onto sulfuric acid: solubilities, diffusivities, and reaction. The Journal of Physical 332 Chemistry, 97(47), 12309–12319. https://doi.org/10.1021/j100149a035 333 Hersbach, H., Bell, B., Berrisford, P., Hirahara, S., Horányi, A., Muñoz-Sabater, J., et al. (2020). 334 335 The ERA5 global reanalysis. *Quarterly Journal of the Royal Meteorological Society*, 146(730), 1999–2049. https://doi.org/10.1002/qj.3803 336 337 Hervig, M. E., Russell, J. M., Gordley, L. L., Daniels, J., Drayson, S. R., & Park, J. H. (1995). 338 Aerosol effects and corrections in the Halogen Occultation Experiment. Journal of 339 Geophysical Research: Atmospheres, 100(D1), 1067–1079. https://doi.org/10.1029/94JD02143 340

341	Kinnison, D. E., Grant, K. E., Connell, P. S., Rotman, D. A., & Wuebbles, D. J. (1994). The
342	chemical and radiative effects of the Mount Pinatubo eruption. Journal of Geophysical
343	Research: Atmospheres, 99(D12), 25705–25731. https://doi.org/10.1029/94JD02318
344	Li, C., Peng, Y., Asher, E., Baron, A. A., Todt, M., Thornberry, T. D., et al. (2024).
345	Microphysical Simulation of the 2022 Hunga Volcano Eruption Using a Sectional
346	Aerosol Model. Geophysical Research Letters, 51(11), e2024GL108522.
347	https://doi.org/10.1029/2024GL108522
348	McCormick, M. P., Steele, H. M., Hamill, P., Chu W. P., & Swissler T. J. (1982). Polar
349	Stratospheric Cloud Sightings by SAM II. Journal of the Atmospheric Sciences, 39(6),
350	1387–1397
351	McHugh, M., Magill, B., Walker, K. A., Boone, C. D., Bernath, P. F., & Russell, J. M. (2005).
352	Comparison of atmospheric retrievals from ACE and HALOE. Geophysical Research
353	Letters, 32(15), 2005GL022403. https://doi.org/10.1029/2005GL022403
354	Millán, L., Santee, M. L., Lambert, A., Livesey, N. J., Werner, F., Schwartz, M. J., et al. (2022).
355	The Hunga Tonga-Hunga Ha'apai Hydration of the Stratosphere. Geophysical Research
356	Letters, 49(13), e2022GL099381. https://doi.org/10.1029/2022GL099381
357	Murphy, D. M., Froyd, K. D., Bourgeois, I., Brock, C. A., Kupc, A., Peischl, J., et al. (2021).
358	Radiative and chemical implications of the size and composition of aerosol particles in
359	the existing or modified global stratosphere. Atmospheric Chemistry and Physics, 21(11)
360	8915-8932. https://doi.org/10.5194/acp-21-8915-2021
361	NASA/LARC/SD/ASDC. (2023). Global Space-based Stratospheric Aerosol Climatology
362	Version 2.21 [Data set]. NASA Langley Atmospheric Science Data Center DAAC.
363	Retrieved from https://doi.org/10.5067/GLOSSAC-L3-V2.21

Ohneiser, K., Ansmann, A., Kaifler, B., Chudnovsky, A., Barja, B., Knopf, D. A., et al. (2022). 364 Australian wildfire smoke in the stratosphere: the decay phase in 2020/2021 and impact 365 on ozone depletion. Atmospheric Chemistry and Physics, 22(11), 7417–7442. 366 https://doi.org/10.5194/acp-22-7417-2022 367 Pardini, F., Burton, M., Arzilli, F., La Spina, G., & Polacci, M. (2018). SO2 emissions, plume 368 369 heights and magmatic processes inferred from satellite data: The 2015 Calbuco eruptions. Journal of Volcanology and Geothermal Research, 361, 12–24. 370 https://doi.org/10.1016/j.jvolgeores.2018.08.001 371 Peterson, D. A., Fromm, M. D., McRae, R. H. D., Campbell, J. R., Hyer, E. J., Taha, G., et al. 372 (2021). Australia's Black Summer pyrocumulonimbus super outbreak reveals potential 373 for increasingly extreme stratospheric smoke events. Npj Climate and Atmospheric 374 Science, 4(1), 38. https://doi.org/10.1038/s41612-021-00192-9 375 Russell, J. M., Gordley, L. L., Park, J. H., Drayson, S. R., Hesketh, W. D., Cicerone, R. J., et al. 376 (1993). The Halogen Occultation Experiment. *Journal of Geophysical Research*: 377 Atmospheres, 98(D6), 10777–10797. https://doi.org/10.1029/93JD00799 378 Santee, M. L., Lambert, A., Froidevaux, L., Manney, G. L., Schwartz, M. J., Millán, L. F., et al. 379 380 (2023). Strong Evidence of Heterogeneous Processing on Stratospheric Sulfate Aerosol in the Extrapolar Southern Hemisphere Following the 2022 Hunga Tonga-Hunga Ha'apai 381 Eruption. Journal of Geophysical Research: Atmospheres, 128(16), e2023JD039169. 382 383 https://doi.org/10.1029/2023JD039169 Santee, M. L., Lambert, A., Manney, G. L., Livesey, N. J., Froidevaux, L., Neu, J. L., et al. 384 (2022). Prolonged and Pervasive Perturbations in the Composition of the Southern 385

386	Hemisphere Midlatitude Lower Stratosphere From the Australian New Year's Fires.
387	Geophysical Research Letters, 49(4). https://doi.org/10.1029/2021GL096270
388	Shi, Q., Jayne, J. T., Kolb, C. E., Worsnop, D. R., & Davidovits, P. (2001). Kinetic model for
389	reaction of ClONO2 with H2O and HCl and HOCl with HCl in sulfuric acid solutions.
390	Journal of Geophysical Research: Atmospheres, 106(D20), 24259–24274.
391	https://doi.org/10.1029/2000JD000181
392	Solomon, S. (1999). Stratospheric ozone depletion: A review of concepts and history. Reviews of
393	Geophysics, 37(3), 275–316. https://doi.org/10.1029/1999RG900008
394	Solomon, S., Dube, K., Stone, K., Yu, P., Kinnison, D., Toon, O. B., et al. (2022). On the
395	stratospheric chemistry of midlatitude wildfire smoke. Proceedings of the National
396	Academy of Sciences, 119(10), e2117325119. https://doi.org/10.1073/pnas.2117325119
397	Solomon, S., Ivy, D. J., Kinnison, D., Mills, M. J., Neely, R. R., & Schmidt, A. (2016).
398	Emergence of healing in the Antarctic ozone layer. Science, 353(6296), 269–274.
399	https://doi.org/10.1126/science.aae0061
400	Solomon, S., Portmann, R. W., Garcia, R. R., Thomason, L. W., Poole, L. R., & McCormick, M.
401	P. (1996). The role of aerosol variations in anthropogenic ozone depletion at northern
402	midlatitudes. Journal of Geophysical Research: Atmospheres, 101(D3), 6713-6727.
403	https://doi.org/10.1029/95JD03353
404	Solomon, S., Stone, K., Yu, P., Murphy, D. M., Kinnison, D., Ravishankara, A. R., & Wang, P.
405	(2023). Chlorine activation and enhanced ozone depletion induced by wildfire aerosol.
406	Nature, 615(7951), 259-264. https://doi.org/10.1038/s41586-022-05683-0

107	Sprenger, M., & Wernli, H. (2015). The LAGRANTO Lagrangian analysis tool – version 2.0.
804	Geoscientific Model Development, 8(8), 2569–2586. https://doi.org/10.5194/gmd-8-2569
109	2015
110	Thomason, L. W. (2012). Toward a combined SAGE II-HALOE aerosol climatology: an
111	evaluation of HALOE version 19 stratospheric aerosol extinction coefficient
112	observations. Atmospheric Chemistry and Physics, 12(17), 8177–8188.
113	https://doi.org/10.5194/acp-12-8177-2012
114	Wang, P. (2024). Data and code for "Contrasting Chlorine Chemistry on Volcanic and Wildfire
115	Aerosols in the Southern Mid-Latitude Lower Stratosphere" [Dataset]. Zenodo.
116	https://doi.org/10.5281/zenodo.13387165
117	Wang, P., Solomon, S., & Stone, K. (2023). Stratospheric chlorine processing after the 2020
118	Australian wildfires derived from satellite data. Proceedings of the National Academy of
119	Sciences, 120(11), e2213910120. https://doi.org/10.1073/pnas.2213910120
120	Wang, X., Randel, W., Zhu, Y., Tilmes, S., Starr, J., Yu, W., et al. (2023). Stratospheric Climate
121	Anomalies and Ozone Loss Caused by the Hunga Tonga-Hunga Ha'apai Volcanic
122	Eruption. Journal of Geophysical Research: Atmospheres, 128(22), e2023JD039480.
123	https://doi.org/10.1029/2023JD039480
124	Wilmouth, D. M., Østerstrøm, F. F., Smith, J. B., Anderson, J. G., & Salawitch, R. J. (2023).
125	Impact of the Hunga Tonga volcanic eruption on stratospheric composition. Proceedings
126	of the National Academy of Sciences, 120(46), e2301994120.
127	https://doi.org/10.1073/pnas.2301994120

428	Wilson, J. C., Atlas, E., Boering, K., Toon, G., Fahey, D., Bui, T. P., et al. (2008). Steady-state
429	aerosol distributions in the extra-tropical, lower stratosphere and the processes that
430	maintain them. Atmos. Chem. Phys.
431	Wohltmann, I., Santee, M. L., Manney, G. L., & Millán, L. F. (2024). The Chemical Effect of
432	Increased Water Vapor From the Hunga Tonga-Hunga Ha'apai Eruption on the Antarctic
433	Ozone Hole. Geophysical Research Letters, 51(4), e2023GL106980.
434	https://doi.org/10.1029/2023GL106980
435	Zhang, J., Kinnison, D., Zhu, Y., Wang, X., Tilmes, S., Dube, K., & Randel, W. (2024).
436	Chemistry Contribution to Stratospheric Ozone Depletion After the Unprecedented
437	Water-Rich Hunga Tonga Eruption. Geophysical Research Letters, 51(7).
438	Zhu, Y., Bardeen, C. G., Tilmes, S., Mills, M. J., Wang, X., Harvey, V. L., et al. (2022).
439	Perturbations in stratospheric aerosol evolution due to the water-rich plume of the 2022
440	Hunga-Tonga eruption. Communications Earth & Environment, 3(1), 248.
441	https://doi.org/10.1038/s43247-022-00580-w

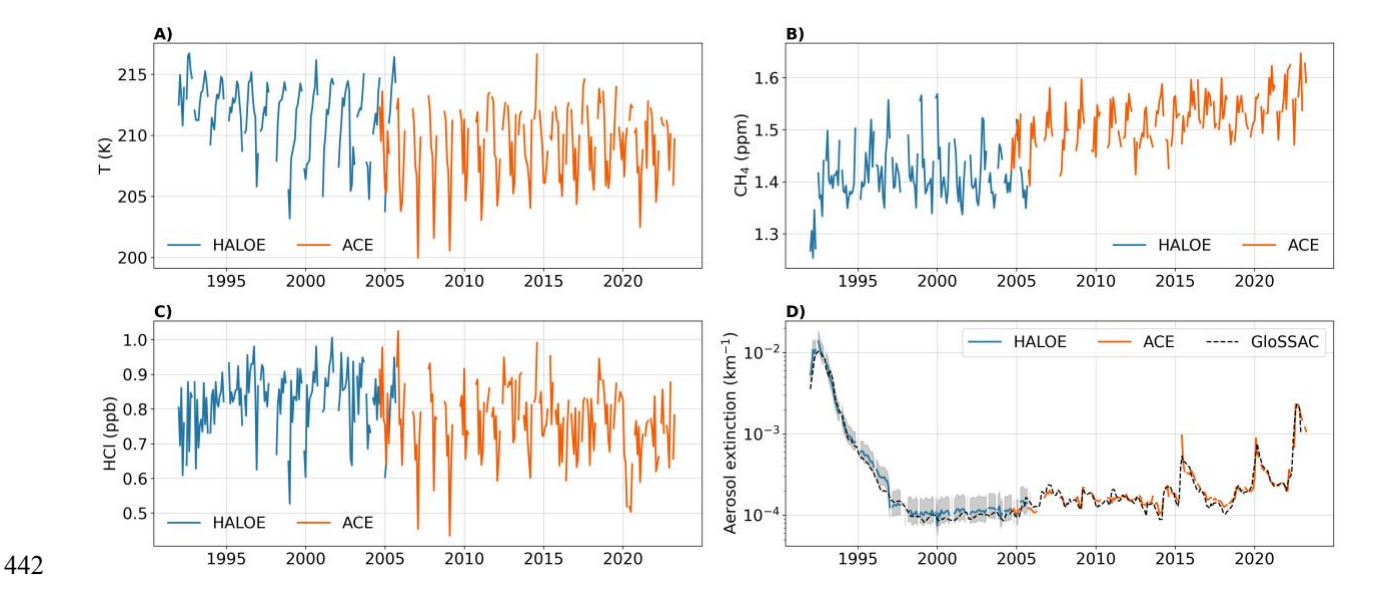


Figure 1. Time series for monthly mean A) temperature, B) CH₄, C) HCl, and D) aerosol extinction in 1992-2005 (from HALOE) and 2004-2023 (from ACE) between 30-45S at 68 hPa. The gray shading in aerosol extinction during the HALOE period represents uncertainty when converting aerosol extinction from 3.45 μ m to 1020 nm (discussed in Section 2.1 in detail). The black dashed line in panel D shows 1020 nm aerosol extinction at 18.5 km from GloSSAC averaged from a similar latitude range.

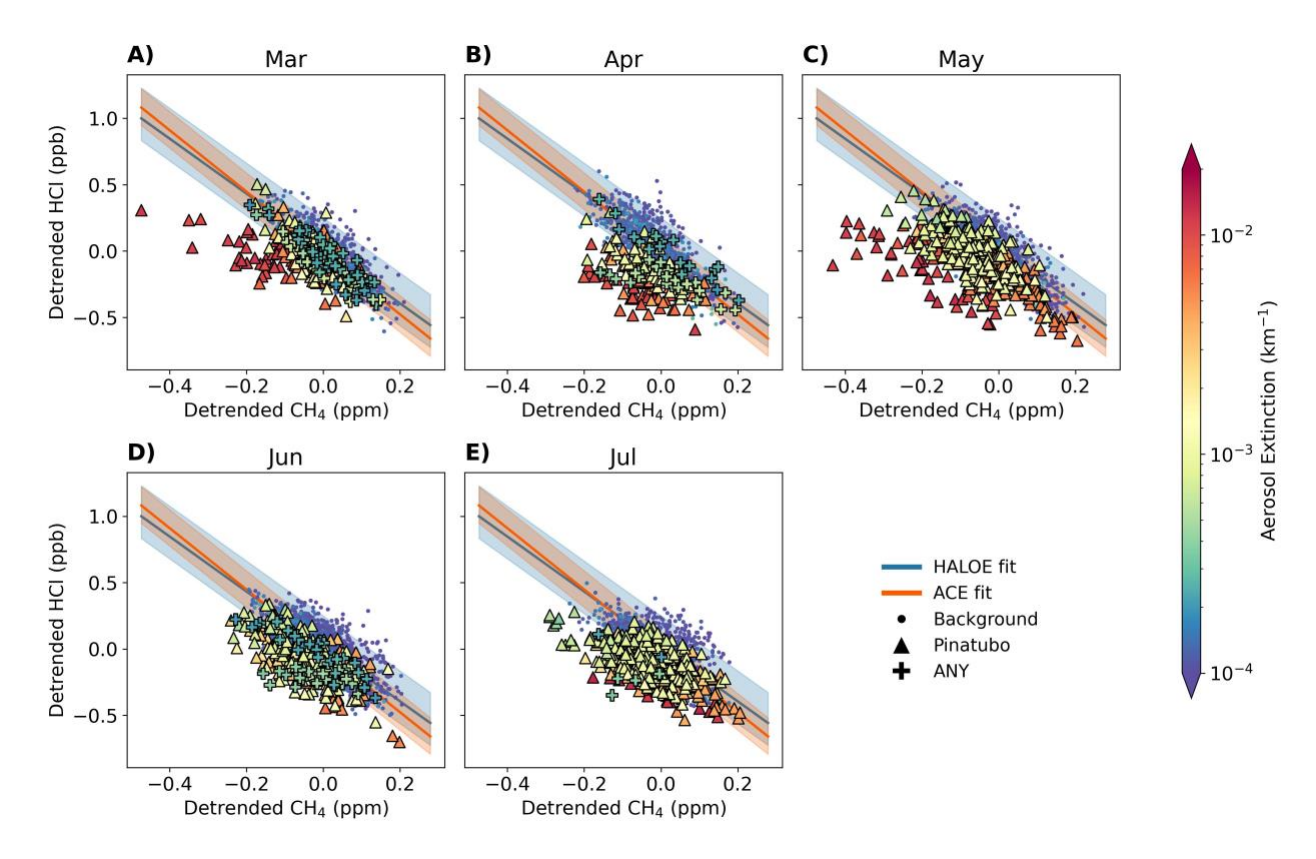


Figure 2. Tracer-tracer scatter plots between detrended CH₄ (x-axis) and detrended HCl (y-axis) color coded by aerosol extinction in HALOE and ACE at 30-45S at 68 hPa. Only the Pinatubo years (1992-1994) and ANY years (2020-2021) are identified by specific markers as they show the most significant changes during each satellite mission (Figure S4 shows these events in separate panels to avoid overlapping points). Shadings indicate a full range of interannual variability (discussed in detail in Section 2.2) for HALOE (in blue) and for ACE (in orange). Note that there is no data coverage at the chosen latitude in May from ACE.

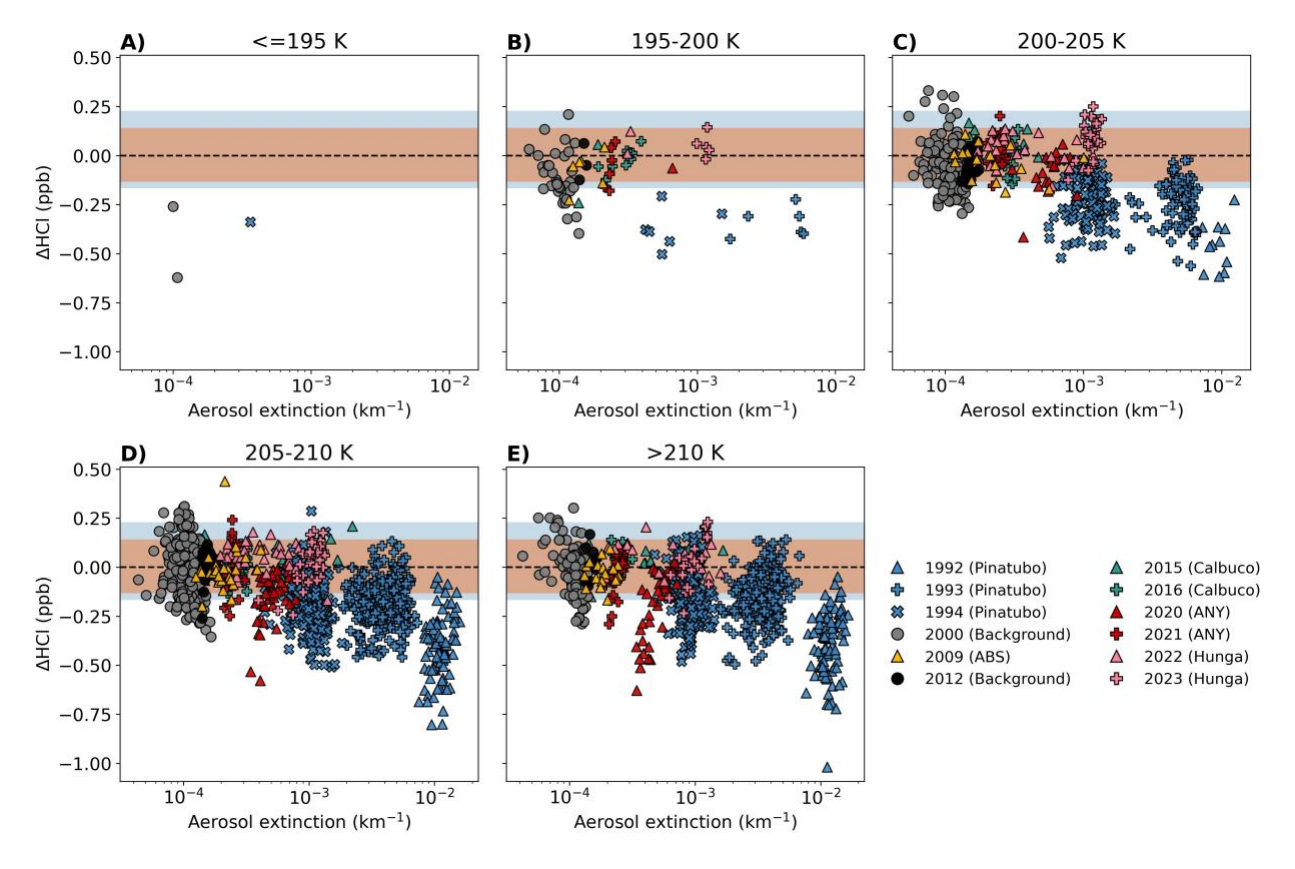


Figure 3. ΔHCl (negative values suggest a net loss in HCl due to chemistry) in 30-45S at 68 hPa as a function of aerosol extinction at individual satellite overpass. Results are grouped in panels showing different temperature ranges (based on 5-day minimum temperatures from the back trajectory calculation for each point, a similar figure but using satellite observed temperature is shown in Figure S2). Two background years, and consecutive years after major volcanic eruptions and the wildfires are highlighted with different markers and colors. The blue and orange shadings surround zero line indicate the full range of interannual variability during the HALOE and ACE periods, respectively.

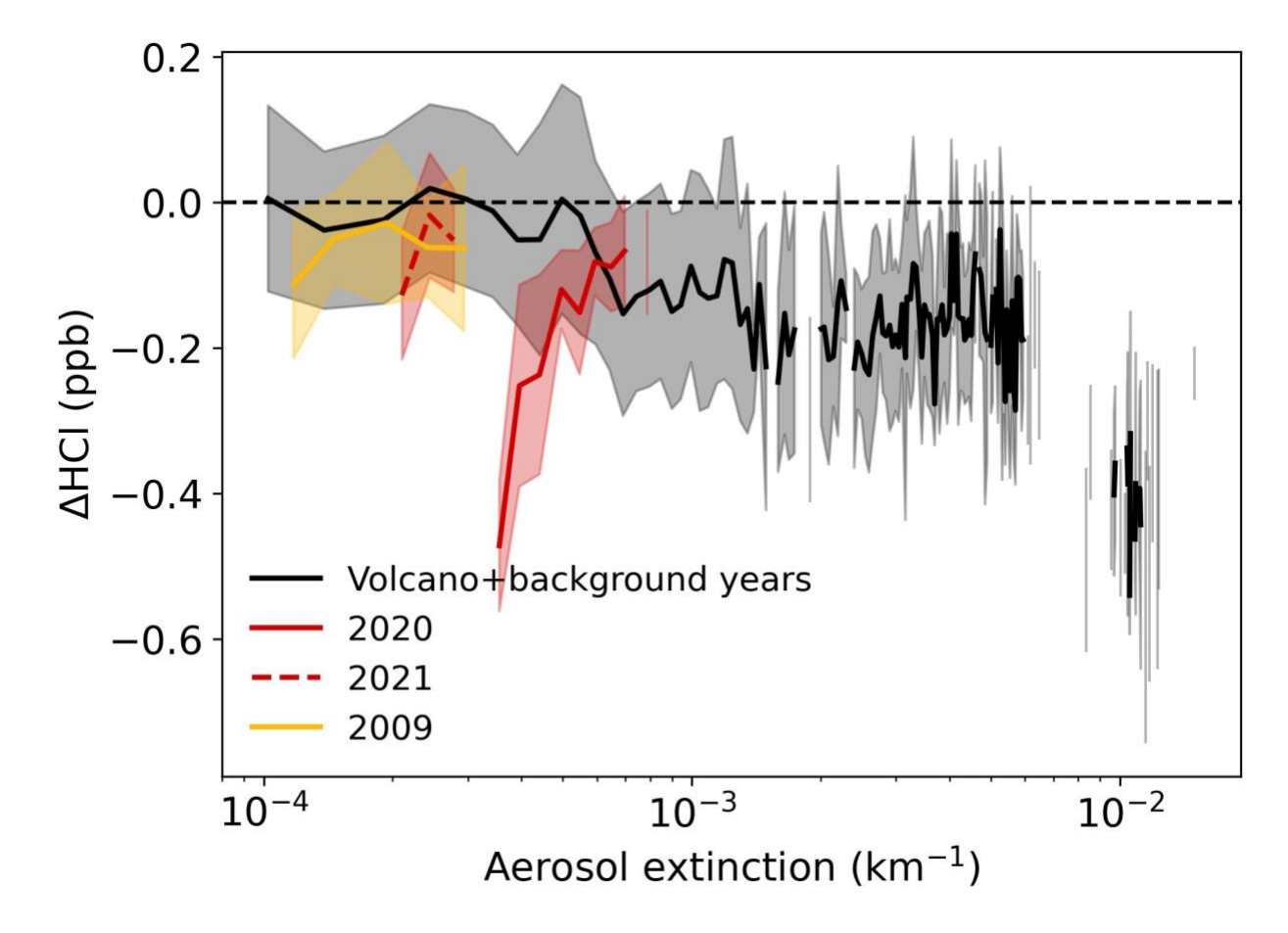


Figure 4. Δ HCl in 30-45S at 68 hPa from 1992 to 2023 binned by aerosol extinction (at every 5×10^{-5} km⁻¹, each bin is averaged by at least 3 data points). The black line shows the averaged net chemical impact on HCl in background and volcanic eruption years. The red lines show the two consecutive years after the ANY fire (solid line for 2020, dashed line for 2021). The yellow line shows the 2009 ABS fire. Color shadings indicate ± 1 standard deviation from the mean for data averaged in each aerosol extinction bin.